



Copper complex supported on the surface of magnetic nanoparticles: an ecofriendly catalyst for C–S and C–Se coupling reactions

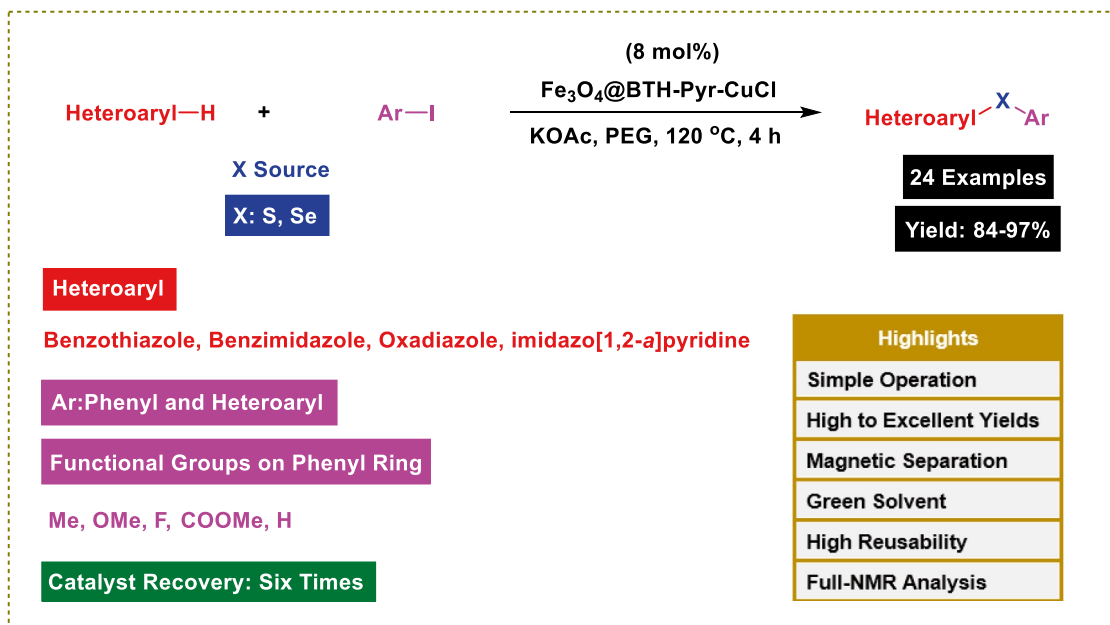
Ke Wang¹ · Li-Yuan Chang²

Received: 24 October 2023 / Accepted: 9 April 2024 / Published online: 27 April 2024
© Iranian Chemical Society 2024

Abstract

Research on the preparation of diallyl sulfides and selenides is always an important challenge among chemists because these compounds are of high biological, pharmaceutical, industrial and chemical importance. For this purpose, in this attractive and highly efficient approach, we wish to report that copper (I) chloride immobilized on magnetic nanoparticles modified with benzothiazole–pyrimidine ligand ($\text{Fe}_3\text{O}_4\text{@BTH-Pyr-CuCl}$) is a novel and efficient magnetically recoverable catalyst for C–S and C–Se bonds formation through reaction of a category of heterocyclic compounds with aryl iodides, sulfur and selenium sources. The structure of $\text{Fe}_3\text{O}_4\text{@BTH-Pyr-CuCl}$ nanocatalyst was well identified with FT-IR, SEM, TEM, EDX, elemental mapping, TGA, XRD, VSM and ICP-OES techniques. The recycling tests confirmed that the $\text{Fe}_3\text{O}_4\text{@BTH-Pyr-CuCl}$ nanocatalyst was reused for 6 times without considerable reduction in its activity. This method is almost better than other methods reported in the literature for C–S and C–Se coupling of heterocycles for the following reasons, such as the use of an environmentally friendly solvent, high yields of products, the use of a catalyst that can be separated and reused and the performance of the reaction in a shorter time, presentation of well-analysis for catalyst and full NMR for products.

Graphical abstract



Keywords $\text{Fe}_3\text{O}_4\text{@BTH-Pyr-CuCl}$ nanocatalyst · C–S bonds · C–Se bonds · Green solvent · High reusability

Extended author information available on the last page of the article

Introduction

The immobilization of catalyst in particular transition metals on the surface of solid supports is one of the popular and efficient strategies in catalysis field [1, 2]. Therefore, choosing a suitable and active solid support plays an important role in the performance of the catalyst [3]. An ideal catalyst from the point of view of green chemistry should have a large active surface and be separable [4]. The high active surface along with the ability to separate the catalyst at the end of the reaction has made nanocatalysts a bridge between homogeneous and heterogeneous catalysts [5–8]. In metallic nanocatalysts, the nanomaterial support and the metal catalyst together form a nanocomposite that is suitable for achieving the best performance [9–13]. Recently, magnetic nanoparticles are widely used as a catalyst support, because these nanoparticles have features such as catalytic capacity, high stability and strength, easy recovery, biocompatibility and low toxicity [14–17]. Magnetic nanoparticles with a core–shell structure form a new type of catalysts, whose shell contains catalytically active species, and the magnetic core acts as a holder that allows separation and recovery of the catalyst [18–20]. One of the most attractive and popular features of magnetic nanocatalysts is the easy separation of this catalyst from the reaction mixture [21, 22]. The catalyst fixed on the magnetic nanoparticles can be easily separated from the reaction medium by an external magnet and can be reused [23–25]. Among the magnetic nanoparticles used as a support for the immobilization of transitional metal complexes as catalyst, Fe_3O_4 nanoparticles are more popular because they are available, their preparation is easier, their surface modification is easily possible, and they have high stability and magnetic properties [25–28].

The formation of carbon–sulfur bonds is an essential step in the preparation of important organic compounds and intermediates [29, 30]. Diaryl sulfides are one of the most important sulfur-containing organic compounds that play a unique role in chemistry, biochemistry, and organic synthesis [31–33]. These compounds are used as multipurpose reagents in organic synthesis and are useful structural parts for the synthesis of sulfur-containing organic compounds [34–36]. Aryl sulfides have shown activities as anti-inflammatory agents, treatment of diabetes, Alzheimer's disease and Parkinson's disease, or as inhibitors for the treatment of human immunodeficiency virus, asthma and obstructive pulmonary disease [37–39]. On the other hand, the synthesis of diaryl selenides has recently become a very attractive and important research field in organic chemistry [40, 41]. Aryl selenides play an important role in medicinal and biological chemistry in particular as anticancer and antiviral drugs [42–45]. The

utilization of sulfur and selenium sources for the C–S and C–Se coupling reactions is one of the most popular and efficient strategies for the preparation of diaryl sulfides and selenides [46]. In the past decades, reactions in which transition metals were used as catalysts have played an important role in the progress of organic chemistry. Copper is one of the most popular and widely used transition metals, which has been recently used for coupling reactions, due to its characteristics such as being cheap, environmentally friendly and having various oxidation states [47, 48].

In this attractive and highly efficient approach, we fabricated copper (I) chloride immobilized on magnetic nanoparticles modified with benzothiazole–pyrimidine ligand ($\text{Fe}_3\text{O}_4@BTH\text{-Pyr-CuCl}$) and evaluated its catalytic activity for the preparation of heteroaryl-aryl sulfides and selenides through reaction of a category of heterocyclic compounds with aryl iodides, sulfur and selenium sources.

Result and discussion

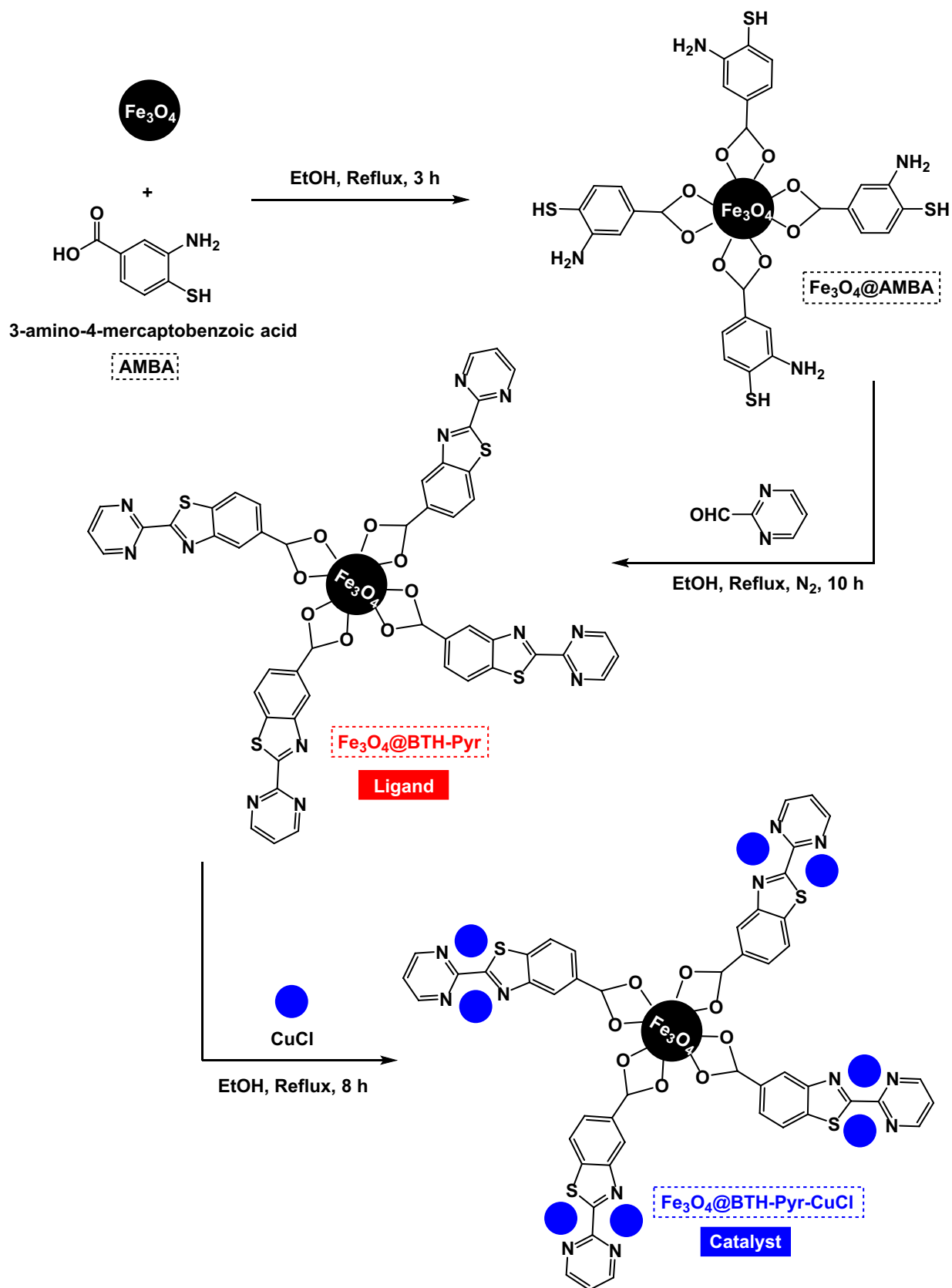
Details of fabrication of $\text{Fe}_3\text{O}_4@BTH\text{-Pyr-CuCl}$ nanocatalyst are shown in Scheme 1. First, magnetic Fe_3O_4 nanoparticles were coated with 3-amino-4-mercaptobenzoic acid in order to prepare the $\text{Fe}_3\text{O}_4@AMBA$ nanocomposite. Next, $\text{Fe}_3\text{O}_4@BTH\text{-Pyr}$ nanomaterial as ligand was prepared through treatment of $\text{Fe}_3\text{O}_4@AMBA$ nanocomposite with pyrimidine-2-carbaldehyde in ethanol under reflux conditions. Finally, CuCl was successfully immobilized on $\text{Fe}_3\text{O}_4@BTH\text{-Pyr}$ ligand in order to fabricate the $\text{Fe}_3\text{O}_4@BTH\text{-Pyr-CuCl}$ nanocatalyst.

Characterization of $\text{Fe}_3\text{O}_4@BTH\text{-Pyr-CuCl}$ nanocatalyst

The structure of $\text{Fe}_3\text{O}_4@BTH\text{-Pyr-CuCl}$ nanocatalyst was well identified with FT-IR, SEM, TEM, EDX, elemental mapping, TGA, XRD, VSM and ICP-OES techniques.

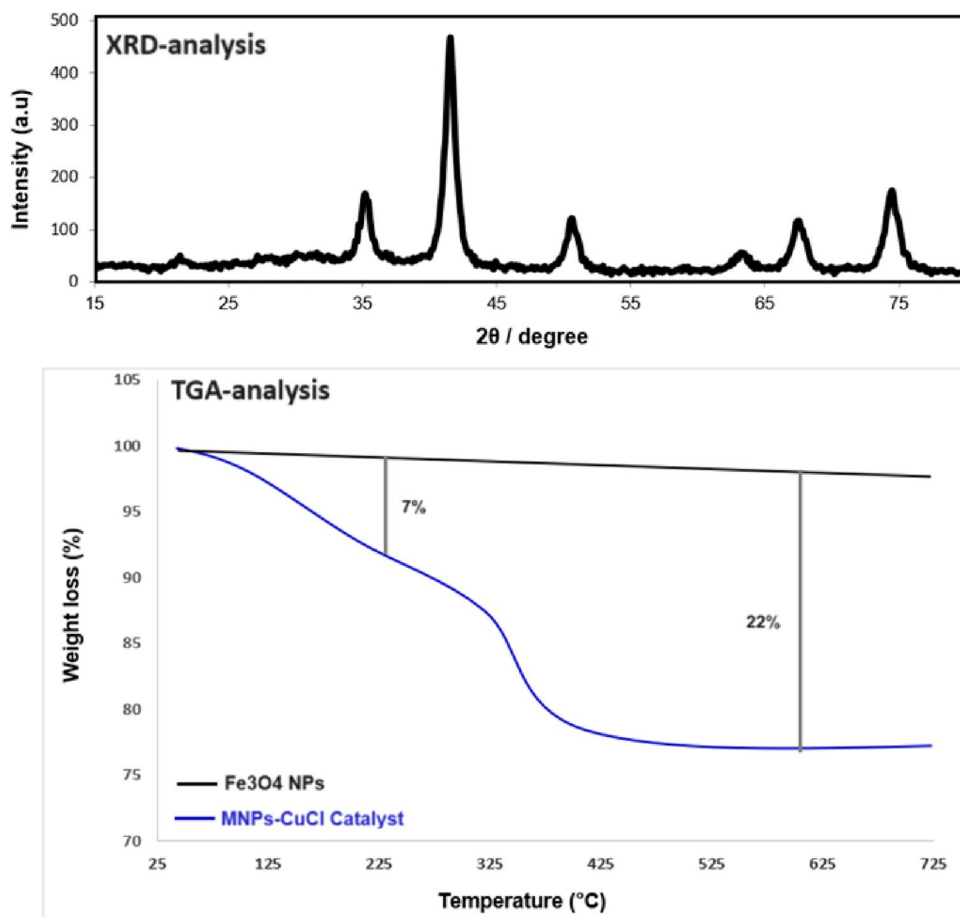
XRD and TGA analysis

In order to study the structure and nature of $\text{Fe}_3\text{O}_4@BTH\text{-Pyr-CuCl}$ nanocatalyst, XRD analysis was used. XRD spectra of $\text{Fe}_3\text{O}_4@BTH\text{-Pyr-CuCl}$ nanocatalyst are shown in Fig. 1. The X-ray analysis of the catalyst is in full agreement with the magnetic analysis of the nanoparticles reported in the references, which indicates that the nature of the $\text{Fe}_3\text{O}_4@BTH\text{-Pyr-CuCl}$ catalyst has not changed despite the immobilization of the functional groups and CuCl on the surface of magnetic Fe_3O_4 nanoparticles [49]. TGA analysis of Fe_3O_4 NPs and $\text{Fe}_3\text{O}_4@BTH\text{-Pyr-CuCl}$ nanocatalyst is shown in Fig. 1. The weight reduction of



Scheme 1 Details of construction of Fe₃O₄@BTH-Pyr-CuCl nanocatalyst

Fig. 1 XRD and TGA analysis of Fe_3O_4 @BTH-Pyr-CuCl nanocatalyst



about 7% to the removal of surface hydroxyl groups and solvents does not affect the surface of the particles. Also, a weight loss of about 15% was observed at the temperature of 225–600 °C, which is related to the decomposition and removal of functional groups and copper complex immobilized on magnetic nanoparticles.

FT-IR spectroscopy

FT-IR spectra of Fe_3O_4 @BTH-Pyr ligand and Fe_3O_4 @BTH-Pyr-CuCl nanocatalyst are shown in Fig. 2. The formation of Fe–O bond is confirmed by an obvious peak at about 570 cm^{-1} in both spectra. The broad peaks at about 3400 cm^{-1} are related to O–H groups on the surface of magnetic nanoparticles. C–H aromatic bonds were also confirmed by several small peaks at about $2800\text{--}3000\text{ cm}^{-1}$. The C–N bond was also confirmed by a characteristic peak at about 1630 cm^{-1} . The peak related to the C–N bond in the Fe_3O_4 @BTH-Pyr ligand appeared in the region of 1662 cm^{-1} , while the same peak in the Fe_3O_4 @BTH-Pyr-CuCl nanocatalyst appeared in the region of 1632 cm^{-1} . The shift of the peak location to the lower region is due to the presence of the ligand bond with the Cu metal.

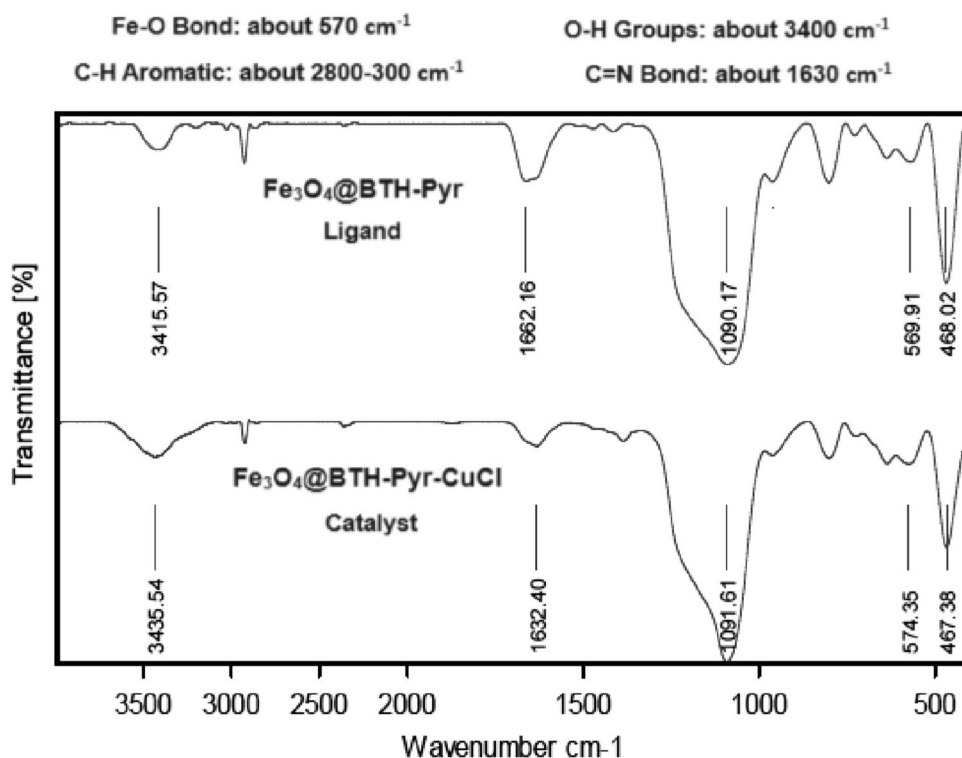
EDX, elemental mapping and ICP-OES spectroscopic techniques

EDX and elemental mapping techniques were used to determine the elements in the structure of the Fe_3O_4 @BTH-Pyr-CuCl catalyst (Fig. 3). The presence of Fe, O, C, N, S and Cu elements in the structure of the Fe_3O_4 @BTH-Pyr-CuCl catalyst was well confirmed by these techniques. ICP-OES analysis was used to find out the amount of copper in the structure of the Fe_3O_4 @BTH-Pyr-CuCl nanocatalyst, and the results showed that the amount of Cu in the structure of the nanocatalyst is $14.25 \times 10^{-5}\text{ mol g}^{-1}$.

SEM and TEM spectroscopic techniques

The morphology and structure of particles in Fe_3O_4 @BTH-Pyr-CuCl nanocatalyst were studied by SEM and TEM photographs (Fig. 4). The SEM and TEM images clearly showed that the formed particles are spherical and uniform and their size is in the range of nanometers. TEM images showed that the particles have a size in the range of 20 nm.

Fig. 2 FT-IR spectra of Fe_3O_4 @BTH-Pyr ligand and Fe_3O_4 @BTH-Pyr-CuCl nanocatalyst



VSM analysis

The magnetic property of all fabricated-nanocomposites for the preparation of the Fe_3O_4 @BTH-Pyr-CuCl nanocatalyst was measured by vibrating-sample magnetometer (VSM) analysis (Fig. 5). Magnetic Fe_3O_4 nanoparticles with a magnetic property of 61.85 (emu g^{-1}) were prepared, and its amount gradually decreased by modifying its surface with 3-amino-4-mercaptobenzoic acid and pyrimidine-2-carbaldehyde. As you can see in Fig. 5, the results showed that the catalyst was prepared with an amount of 45.875 (emu g^{-1}), which is a high amount and indicates the high magnetic property of this synthesized nanocatalyst.

Catalytic investigation of Fe_3O_4 @BTH-Pyr-CuCl in C-H arylation

First the reaction of benzo[d]thiazole, iodobenzene and S_8 as sulfur source for the preparation of 2-(phenylthio)benzo[d]thiazole (product 4a) was considered as the sample reaction for the optimization of conditions. In the absence of catalyst, the product 4a was not formed in the presence of KOH in DMF (Table 1, Entry 1). By using Fe_3O_4 @BTH-Pyr-CuCl catalyst, the progress of the reaction increased significantly. By increasing the amount of the Fe_3O_4 @BTH-Pyr-CuCl catalyst up to 8 mol%, the yield of the desired product also increased, but no change in the yield was seen at amounts higher than 8 mol% (9 and 10 mol% of the catalyst). Therefore, the amount of 8 mol% of the Fe_3O_4 @BTH-Pyr-CuCl

catalyst was chosen as the optimal amount (Table 2, Entry 5). The presence of base in the reaction had a great effect on the reaction because in the absence of base the desired reaction did not take place (Table 2, Entry 1). Among tested bases, the best results were seen in the presence of KOAc as base (Table 2, Entry 9). Finally, in order to select the best medium reaction, a number of solvents were tested under the optimized amount of Fe_3O_4 @BTH-Pyr-CuCl nanocatalyst in the presence of KOAc as base. The results confirmed that PEG is the best solvent for the preparation of 2-(phenylthio)benzo[d]thiazole (product 4a) (Table 3, Entry 6). The yield of the obtained product 4a decreased at a temperature lower than 120 $^\circ\text{C}$ (Table 3, Entry 7), while temperatures above 120 $^\circ\text{C}$ did not affect the efficiency and progress of the reaction (Table 3, Entries 8–9). Only, 10% of the model product was obtained in the absence of solvent after 12 h (Table 3, Entry 10).

In next stage of experimental works, we decide to study the scope of various heterocyclic compounds and aryl or heteroaryl iodides for synthesis of heteroaryl-aryl and di-heteroaryl sulfides and selenides catalyzed by Fe_3O_4 @BTH-Pyr-CuCl nanomaterial (8 mol%) in the presence of KOAc in PEG at 120 $^\circ\text{C}$ for 4 h (Table 4). The obtained results clearly showed that this catalytic system is very efficient because different derivatives of the heteroaryl-aryl and di-heteroaryl sulfide and selenide products were synthesized with high yields under the described conditions. One of the attractions of this method is that various derivatives of heterocyclic sulfides and selenides can be easily synthesized by

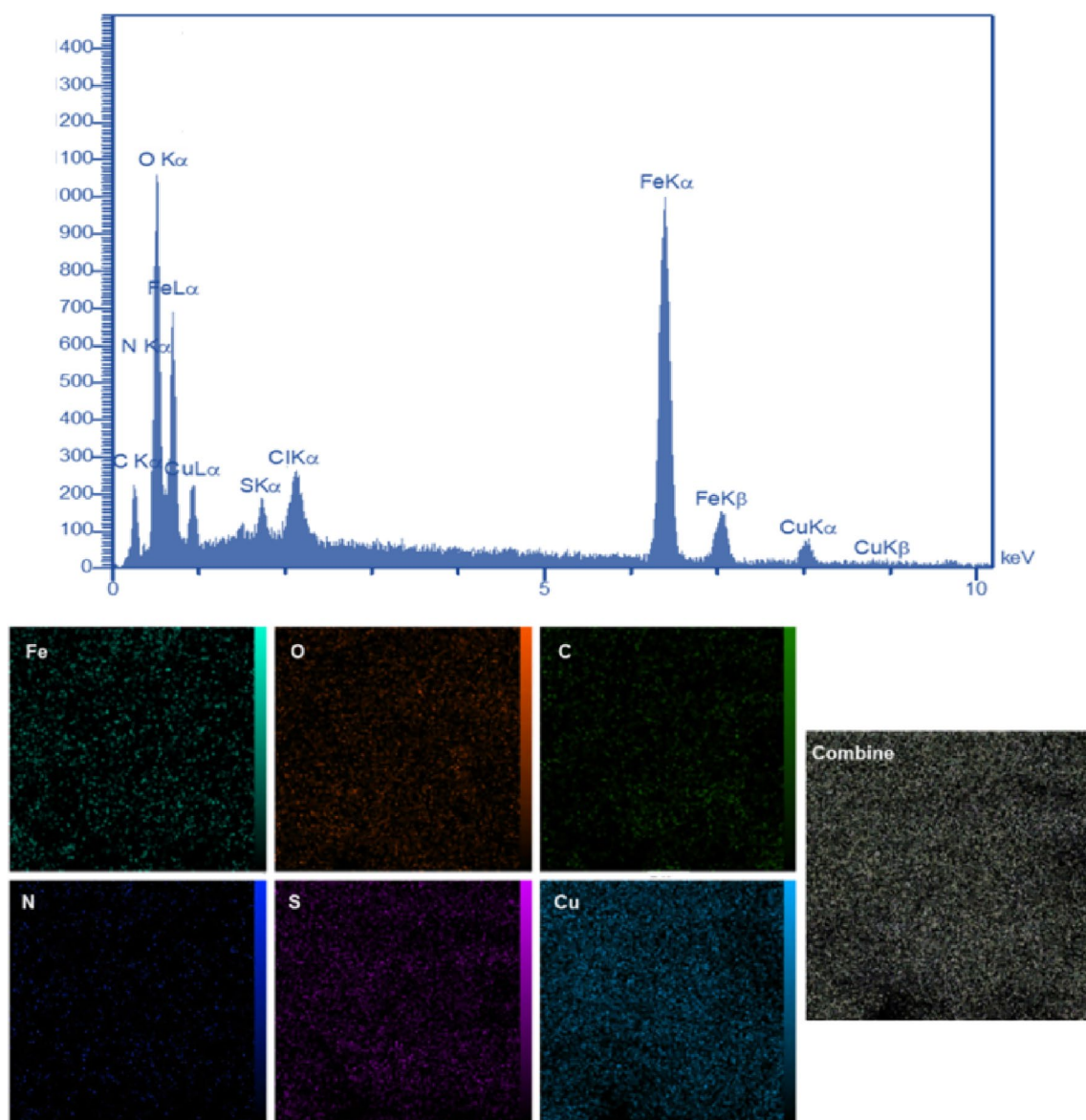


Fig. 3 EDX and elemental mapping analysis of $\text{Fe}_3\text{O}_4@\text{BTH-Pyr-CuCl}$ nanocatalyst

this catalytic system. Although all the obtained heteroaryl-aryl and di-heteroaryl sulfide and selenides products are known and previously reported, synthesis of this number of heteroaryl-aryl and di-heteroaryl sulfides has never been reported by any methods.

In order to study reusability of $\text{Fe}_3\text{O}_4@\text{BTH-Pyr-CuCl}$ nanocatalyst in this methodology, the reaction of benzo[d]thiazole, iodobenzene and S_8 as sulfur source for the preparation of 2-(phenylthio)benzo[d]thiazole (product 4a) was considered as the sample reaction. After the compilation of

the reaction, $\text{Fe}_3\text{O}_4@\text{BTH-Pyr-CuCl}$ nanocatalyst was easily separated with an external magnet (washed several times with ethyl acetate and reused for next runs. As shown in Fig. 6, the $\text{Fe}_3\text{O}_4@\text{BTH-Pyr-CuCl}$ nanocatalyst was reused for 6 times without considerable reduction in its activity. As shown in Fig. 6, VSM analysis of the reused $\text{Fe}_3\text{O}_4@\text{BTH-Pyr-CuCl}$ nanocatalyst after 6 times has still high magnetic nature ($43.524 \text{ emu g}^{-1}$). ICP-OES analysis was also used to find out the amount of copper in the structure of the reused $\text{Fe}_3\text{O}_4@\text{BTH-Pyr-CuCl}$ nanocatalyst after 6 times, and the

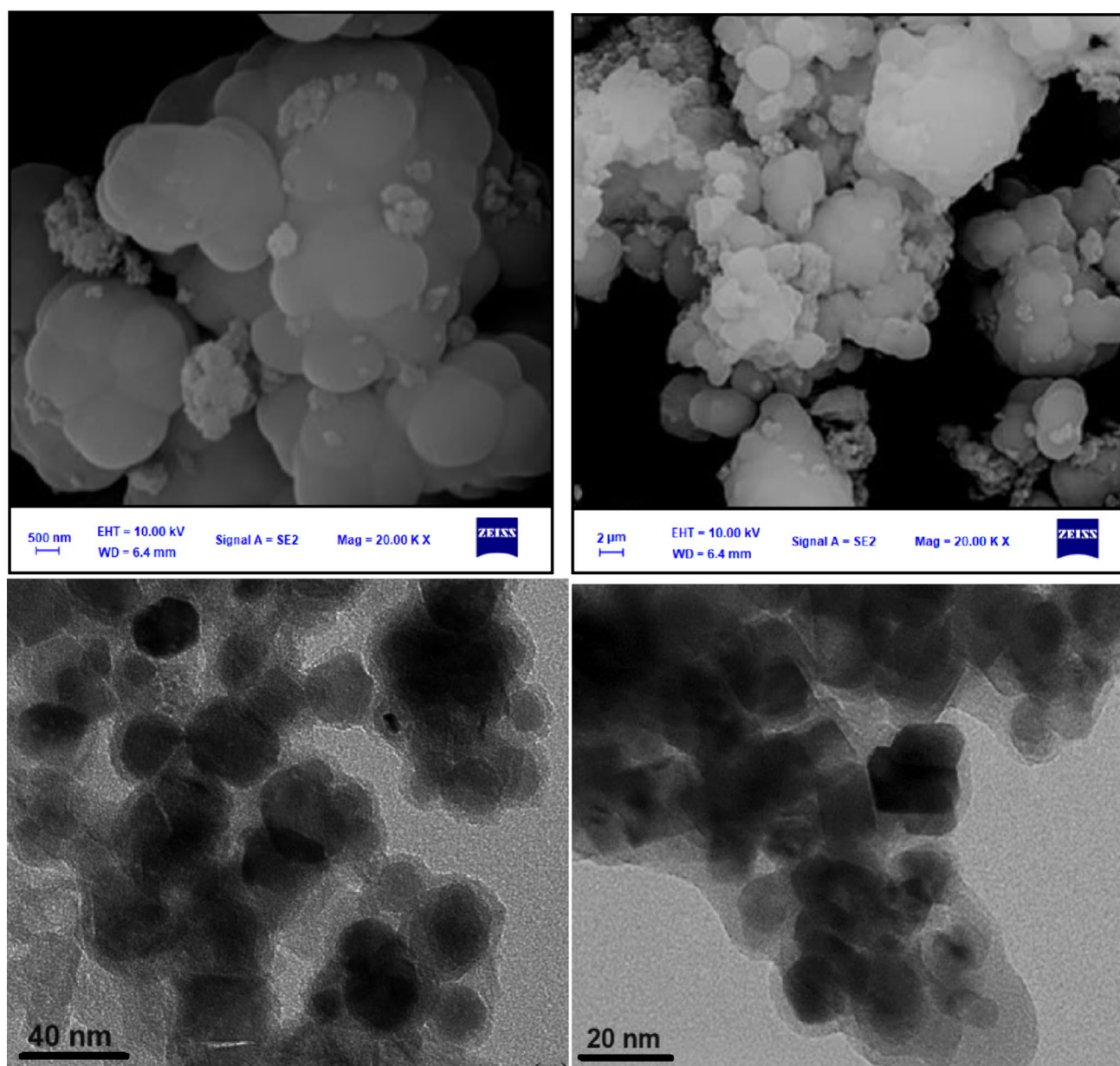


Fig. 4 SEM and TEM images of $\text{Fe}_3\text{O}_4@\text{BTH-Pyr-CuCl}$ nanocatalyst

results showed that the amount of Cu in the structure of the nanocatalyst is $14.19 \times 10^{-5} \text{ mol g}^{-1}$.

In order to investigate the efficiency of $\text{Fe}_3\text{O}_4@\text{BTH-Pyr-CuCl}$ nanocatalyst for C–S coupling heterocycles, we compared the results of this methodology with other reported methods in the literature for the preparation of 2-(phenylthio)benzo[d]thiazole (product 4a) as the template reaction. As

shown in Table 5, this method is more preferable than other methods, such as the use of an environmentally friendly solvent, high product yield, the use of a catalyst that can be separated and reused, the use of milder conditions and the performance of the reaction in a shorter time.

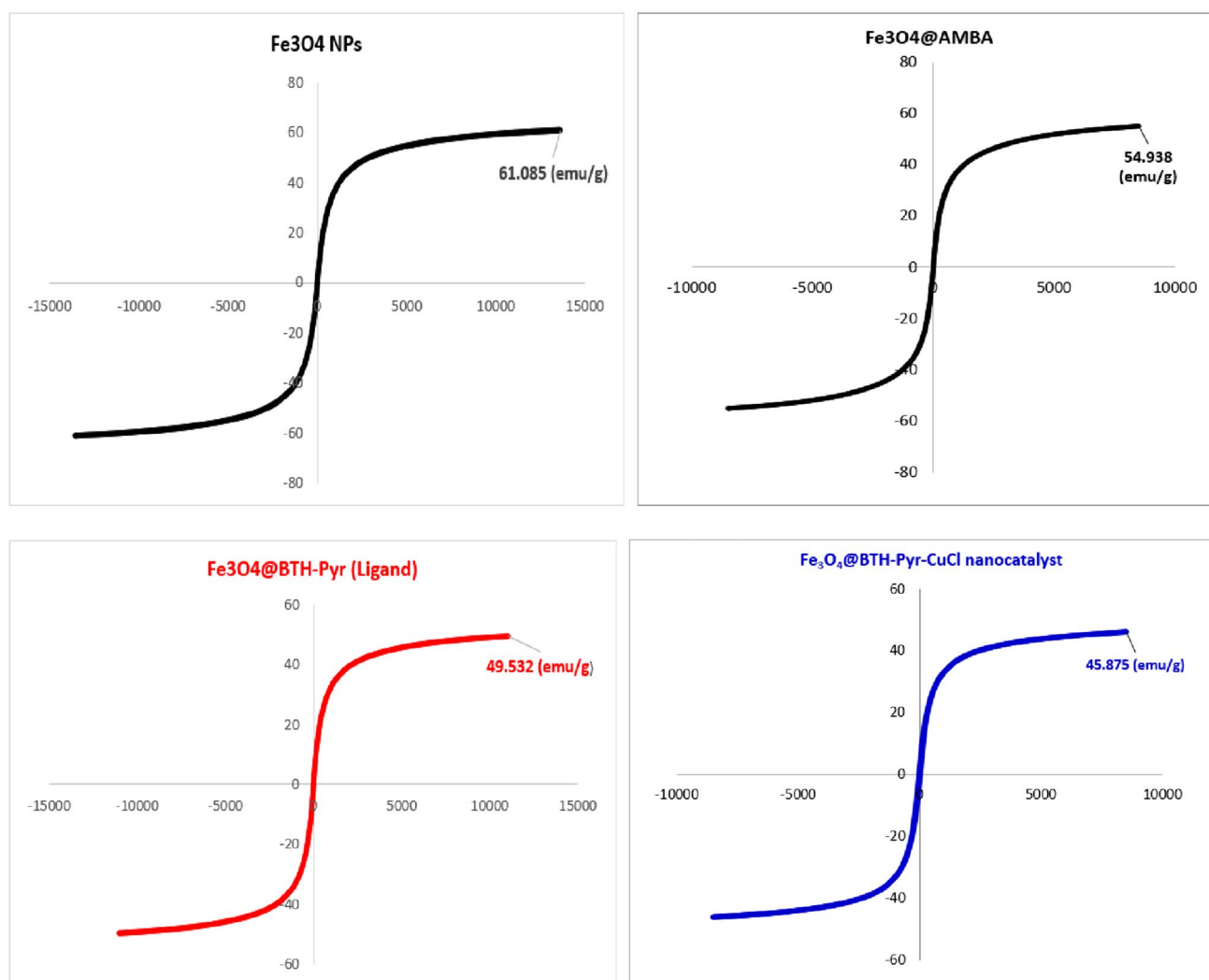


Fig. 5 VSM analysis of Fe_3O_4 NPs, Fe_3O_4 @AMBA, Fe_3O_4 @BTH-Pyr ligand and Fe_3O_4 @BTH-Pyr-CuCl nanocatalyst

Conclusion

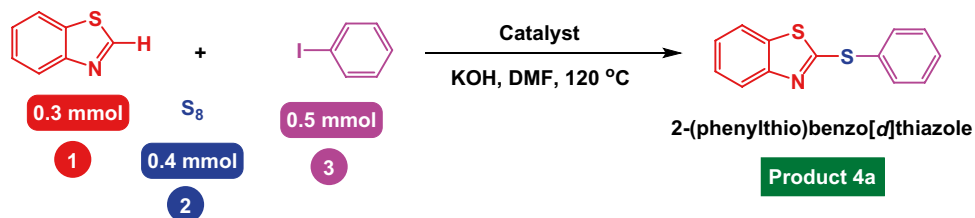
In summary, we constructed a novel magnetically recoverable copper nanocatalyst through copper (I) chloride immobilized on magnetic nanoparticles modified with benzothiazole–pyrimidine ligand (Fe_3O_4 @BTH-Pyr-CuCl) and studied its catalytic activities in preparation of heteroaryl-aryl sulfides and selenides. One-pot three-component reactions of reaction of a category of heterocyclic compounds with aryl iodides, sulfur and selenium sources were successfully catalyzed by Fe_3O_4 @BTH-Pyr-CuCl nanocomposite and the desired aryl sulfide and selenide products were afforded with high yields. The recycling

tests confirmed that the Fe_3O_4 @BTH-Pyr-CuCl nanocatalyst was reused for 6 times without considerable reduction in its activity.

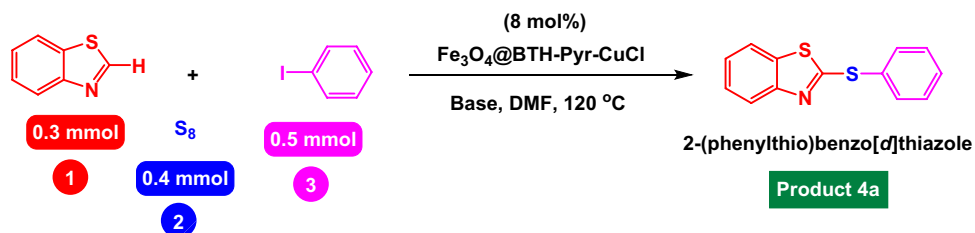
Experimental

General procedure for preparation of C–S and C–Se bonds formation catalyzed by Fe_3O_4 @BTH-Pyr-CuCl nanocomposite

In a round bottomed flask, a mixture of aryl iodides (0.5 mmol), sulfur or selenium source (0.4 mmol), KOAc

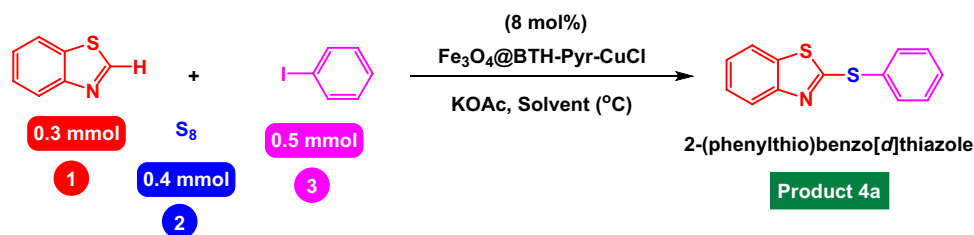
Table 1 Effect of catalyst on the preparation of 2-(phenylthio)benzo[d]thiazole (Product 4a)

Entry	Catalyst (mol%)	Time (h)	Yield % ^a
1	No catalyst	24	×
2	Fe ₃ O ₄ @BTH-Pyr-CuCl (5 mol%)	4	72
3	Fe ₃ O ₄ @BTH-Pyr-CuCl (6 mol%)	4	79
4	Fe ₃ O ₄ @BTH-Pyr-CuCl (7 mol%)	4	84
5	Fe ₃ O ₄ @BTH-Pyr-CuCl (8 mol%)	4	87
6	Fe ₃ O ₄ @BTH-Pyr-CuCl (9 mol%)	4	87
7	Fe ₃ O ₄ @BTH-Pyr-CuCl (10 mol%)	4	87

^aYields referred to isolated products**Table 2** Effect of several base on the preparation of 2-(phenylthio)benzo[d]thiazole (Product 4a)

Entry	Base	Time (h)	Yield % ^a
1	No base	24	×
2	KOH	4	87
3	K ₂ CO ₃	4	84
4	NaOH	4	58
5	DBU	4	51
6	t-BuOK	4	44
7	Et ₃ N	4	84
8	Na ₂ CO ₃	4	80
9	KOAc	4	92

^aYields referred to isolated products

Table 3 Influence of solvent on the preparation of 2-(phenylthio)benzo[d]thiazole (Product 4a)

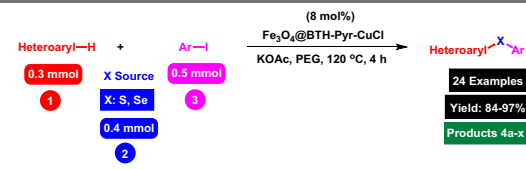
Entry	Solvent ($^{\circ}\text{C}$)	Time (h)	Yield % ^a
1	DMF (100 $^{\circ}\text{C}$)	4	92
2	EtOH (Reflux)	4	77
3	Toluene (120 $^{\circ}\text{C}$)	4	34
4	DMSO (120 $^{\circ}\text{C}$)	4	88
5	Anisole (120 $^{\circ}\text{C}$)	4	89
6	PEG (120 $^{\circ}\text{C}$)	4	95
7	PEG-400 (110 $^{\circ}\text{C}$)	4	92
8	PEG-400 (130 $^{\circ}\text{C}$)	4	95
9	PEG-400 (140 $^{\circ}\text{C}$)	4	95
10	Solvent-Free (100 $^{\circ}\text{C}$)	12	10

^aYields referred to isolated products

(2 equiv) and $\text{Fe}_3\text{O}_4\text{@BTH-Pyr-CuCl}$ catalyst (8 mol%) was stirred in PEG-400 at 120 $^{\circ}\text{C}$. After 30 min, heteroaryls (0.3 mmol) were added to reaction mixture and stirred for 4 h. (The progress of the reaction was monitored by thin-layer chromatography (TLC).) After completion of the reaction, the $\text{Fe}_3\text{O}_4\text{@BTH-Pyr-CuCl}$ was magnetically separated and reaction mixture was cooled to room temperature and H_2O (4 mL) was added. The product was extracted with

EtOAc (3 \times 4 mL) and dried over anhydrous Na_2SO_4 . The crude material was purified with chromatography column on silica gel (EtOAc/*n*-hexane) which gives the heteroaryl-aryl and di-heteroaryl sulfides products with 84–97%. All heteroaryl-aryl and di-heteroaryl sulfide and selenide products are previously reported and known [35, 55–64]. HNMR and CNMR were used in order to identify the structure of the heteroaryl-aryl and di-heteroaryl sulfide products.

Table 4 Scope of $\text{Fe}_3\text{O}_4@$ BTH-Pyr-CuCl nanocatalyst in synthesis of heteroaryl-aryl and di-heteroaryl sulfides and selenides



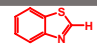
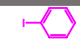
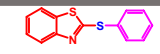
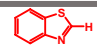
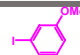
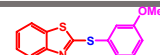
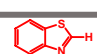
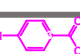
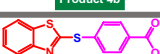
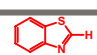







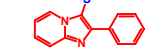
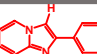
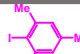
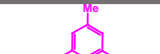


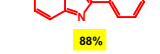
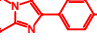
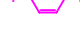
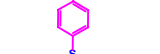






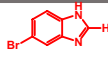
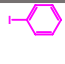
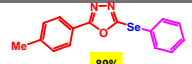
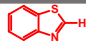
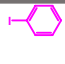

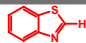
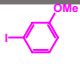

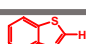
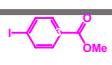
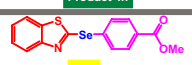
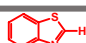
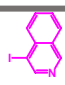

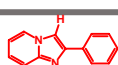
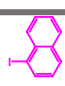
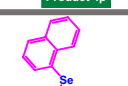
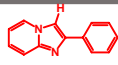
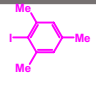
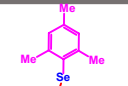
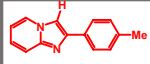
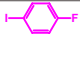
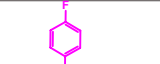
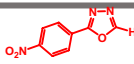
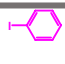
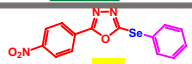
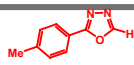
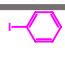
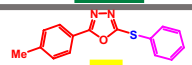
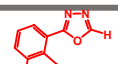
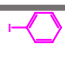
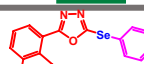
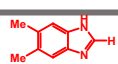
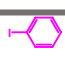
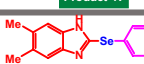
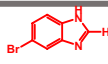
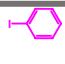
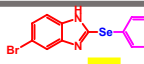
Entry	Aryl Iodide	Heterocycles	Products
1			 95% Product 4a
2			 97% Product 4b
3			 89% Product 4c
4			 92% Product 4d
5			 91% Product 4e
6			 88% Product 4f
7			 85% Product 4g
8			 87% Product 4h
9			 88% Product 4i
10			 89% Product 4j
11			 88% Product 4k

Table 4 (continued)

12			 89% Product 4u
13			 94% Product 4m
14			 97% Product 4n
15			 86% Product 4o
16			 93% Product 4p
17			 88% Product 4q
18			 87% Product 4r
19			 85% Product 4s
20			 85% Product 4t
21			 89% Product 4u
22			 85% Product 4v
23			 84% Product 4w
24			 86% Product 4x

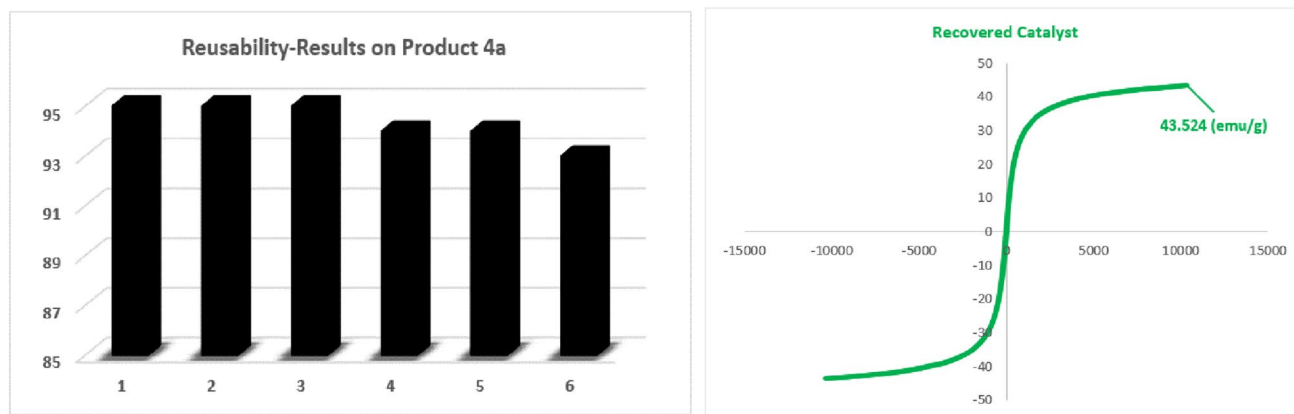
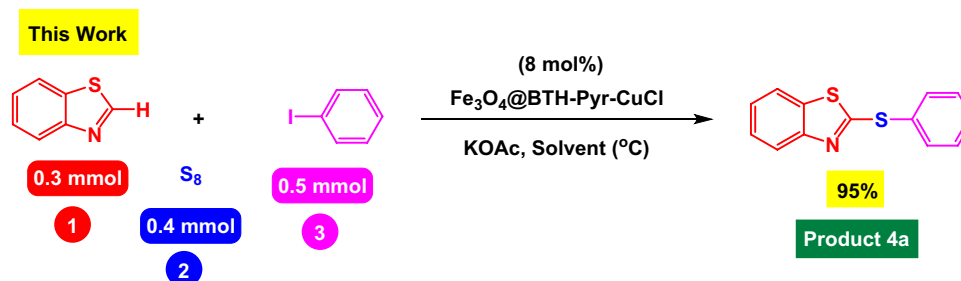


Fig. 6 Reusability-results of $\text{Fe}_3\text{O}_4@\text{BTH-Pyr-CuCl}$ nanocatalyst and VSM analysis of the recovered $\text{Fe}_3\text{O}_4@\text{BTH-Pyr-CuCl}$ nanocatalyst

Table 5 Compression of efficiency of this methods with other methods for synthesis of 2-(phenylthio)benzo[d]thiazole (product 4a)



Entry	Catalyst	Conditions	Yield% [Ref]
1	$\text{Cu}(\text{OAc})_2 \cdot \text{H}_2\text{O}$ (20 mol%)	1,4.dioxane, 100 $^\circ\text{C}$, 5 h	77 [50]
2	TMS_3SiH , AIBN (5 mol%)	Toluene, 110 $^\circ\text{C}$, 4 h	90 [51]
3	$\text{NiCl}_2 \cdot 6\text{H}_2\text{O}$, Bpy, Zn powder	Et_3N , Ball milling, 30 Hz, 2 h	82 [52]
4	CuI , cyclohexane-1,2-diamine	K_2CO_3 , DMSO, 120 $^\circ\text{C}$, 8 h	86 [53]
5	CuI , BiPy	Na_2CO_3 , DMF, 140 $^\circ\text{C}$, 24 h	90 [54]
6	CuO	K_2CO_3 , DMF, 140 $^\circ\text{C}$, 24 h	78 [43]

Supplementary Information The online version contains supplementary material available at <https://doi.org/10.1007/s13738-024-03015-9>.

References

- A.K. Sharma, H. Joshi, A.K. Singh, *RSC Adv.* **10**, 6452 (2020)
- Y. Zhang, N. Song, *Biol. Mol. Chem.* **1**, 53 (2023)
- V.G. Pandya, S.B. Mhaske, *Org. Lett.* **16**, 3836 (2014)
- R. Chawla, L.D.S. Yadav, *Org. Biomol. Chem.* **17**, 4761 (2019)
- S. Gupta, *J. Synth. Chem.* **1**, 16 (2022)
- M. Kazemi, *Nanomater. Chem.* **1**, 1 (2023)
- S. Vajar, M. Mokhtary, *Polycycl. Aromat. Compd.* **39**, 111 (2019)
- E. Doustkhah, S. Rostamnia, M. Imura, Y. Ide, S. Mohammadi, C.J.T. Hyland, J. You, N. Tsunoji, B. Zeynizadeh, Y. Yamauchi, *RSC Adv.* **7**, 56306 (2017)
- R. Deilam, F. Moeinpour, F.S. Mohseni-Shahri, *Monatshefte Für Chemie - Chem. Mon.* **151**, 1153 (2020)
- M. Ghobadi, *J. Synth. Chem.* **1**, 84 (2022)
- M. Ghobadi, M. Kargar Razi, R. Javahershenas, M. Kazemi, *Synth. Commun.* **51**, 647 (2021)
- S. Rostamnia, E. Doustkhah, R. Bulgar, B. Zeynizadeh, *Microporous Mesoporous Mater.* **225**, 272 (2016)
- S. Rostamnia, K. Lamei, F. Pourhassan, *RSC Adv.* **4**, 59626 (2014)
- P. Ghamari Kargar, C. Len, R. Luque, *Sustain. Chem. Pharm.* **27**, 100672 (2022)
- R. Arundhathi, D. Damodara, P.R. Likhar, M.L. Kantam, P. Saravanan, T. Magdaleno, S.H. Kwon, *Adv. Synth. Catal.* **353**, 1591 (2011)
- L.S. Ardakani, A. Arabmarkadeh, M. Kazemi, *Synth. Commun.* **51**(6), 856–879 (2021)

17. R. Taghavi, S. Rostamnia, M. Farajzadeh, H. Karimi-Maleh, J. Wang, D. Kim, H.W. Jang, R. Luque, R.S. Varma, M. Shokouhimehr, *Inorg. Chem.* **61**, 15747 (2022)
18. F.M. Moghaddam, M. Eslami, *Appl. Organomet. Chem.* **32**, e4463 (2018)
19. M.R. Abdi, *Biol. Mol. Chem.* **1**, 1 (2023)
20. A. Baghban, M. Heidarizadeh, E. Doustkhah, S. Rostamnia, P.F. Rezaei, *Int. J. Biol. Macromol.* **103**, 1194 (2017)
21. A.R. Sardarian, F. Mohammadi, M. Esmailpour, *Res. Chem. Intermed.* **45**, 1437 (2019)
22. E. Doustkhah, M. Heidarizadeh, S. Rostamnia, A. Hassankhani, B. Kazemi, X. Liu, *Mater. Lett.* **216**, 139 (2018)
23. R. Eisavi, A. Karimi, *RSC Adv.* **9**, 29873 (2019)
24. M. Kazemi, *Synth. Commun.* **50**, 1899 (2020)
25. J. Hou, M. Kazemi, *Res. Chem. Intermed.* **50**, 1845–1872 (2024)
26. A. Noory Fajer, H. Khabt Aboud, H.A. Al-Bahrani, M. Kazemi, *Polycycl. Aromat. Compd.* **43**, 1–47 (2023). <https://doi.org/10.1080/10406638.2023.2255723>
27. M. Lakshman, *J. Synth. Chem.* **1**, 48 (2022)
28. S. Sajjadifar, M.A. Zolfigol, F. Tami, *J. Chinese Chem. Soc.* **66**, 307 (2019)
29. K. Takagi, *Chem. Lett.* **16**, 2221 (1987)
30. L. Shiri, A. Ghorbani-Choghamarani, M. Kazemi, *Aust. J. Chem.* **69**, 585 (2016)
31. M. Kazemi, *Synth. Commun.* **50**, (2020).
32. I.M. Yonova, C.A. Osborne, N.S. Morrisette, E.R. Jarvo, *J. Org. Chem.* **79**, 1947 (2014)
33. P. Anbarasan, H. Neumann, M. Beller, *Chem. Commun.* **47**, 3233 (2011)
34. X. Li, T. Yuan, Y. Yang, J. Chen, *Tetrahedron* **70**, 9652 (2014)
35. L.-F. Niu, Y. Cai, C. Liang, X.-P. Hui, P.-F. Xu, *Tetrahedron* **67**, 2878 (2011)
36. R. Zhang, H. Ding, X. Pu, Z. Qian, Y. Xiao, *Catalysts* **10**, 1339 (2020)
37. M. Vaddamanu, K. Velappan, G. Prabusankar, *New J. Chem.* **44**, 129 (2020)
38. M. Arisawa, T. Ichikawa, M. Yamaguchi, *Org. Lett.* **14**, 5318 (2012)
39. C.C. Eichman, J.P. Stambuli, *Molecules* **16**, 590 (2011)
40. X. Xu, W. Wang, L. Lu, J. Zhang, J. Luo, *Catal. Letters* **152**, 3031 (2022)
41. V. Rathore, S. Kumar, *Green Chem.* **21**, 2670 (2019)
42. Y. Kobiki, S. Kawaguchi, T. Ohe, A. Ogawa, *Beilstein J. Org. Chem.* **9**, 1141 (2013)
43. A.R. Rosario, K.K. Casola, C.E.S. Oliveira, G. Zeni, *Adv. Synth. Catal.* **355**, 2960 (2013)
44. G. Kumaraswamy, V. Ramesh, M. Gangadhar, S. Vijaykumar, *Asian J. Org. Chem.* **7**, 1689 (2018)
45. H. Chuai, S.-Q. Zhang, H. Bai, J. Li, Y. Wang, J. Sun, E. Wen, J. Zhang, M. Xin, *Eur. J. Med. Chem.* **223**, 113621 (2021)
46. D. Hu, M. Liu, H. Wu, W. Gao, G. Wu, *Org. Chem. Front.* **5**, 1352 (2018)
47. X. Liu, S.-B. Zhang, H. Zhu, Z.-B. Dong, *J. Org. Chem.* **83**, 11703 (2018)
48. L. Chen, A. Noory Fajer, Z. Yessimbekov, M. Kazemi, M. Mohammadi, *J. Sulfur Chem.* **40**, 451 (2019)
49. M.M. Khodaei, A. Alizadeh, M. Haghypour, *Res. Chem. Intermed.* **45**, 2727 (2019)
50. G. Balakishan, G. Kumaraswamy, V. Narayanarao, P. Shankaraiah, *Heterocycl. Commun.* **27**, 17 (2021)
51. D. Kumar, B.B. Mishra, V.K. Tiwari, *J. Org. Chem.* **79**, 251 (2014)
52. X. Hao, D. Feng, H. Chen, P. Huang, F. Guo, *Chem.—A Eur. J.* **29**(60), e202302119 (2023)
53. V.N. Bochatay, P.J. Boissarie, J.A. Murphy, C.J. Suckling, S. Lang, *J. Org. Chem.* **78**, 1471 (2013)
54. S. Ranjit, R. Lee, D. Heryadi, C. Shen, J. Wu, P. Zhang, K.-W. Huang, X. Liu, *J. Org. Chem.* **76**, 8999 (2011)
55. P. Gandeepan, J. Mo, L. Ackermann, *Chem. Commun.* **53**, 5906 (2017)
56. J. Rafique, G. Farias, S. Saba, E. Zapp, I.C. Bellettini, C.A. Momoli Salla, I.H. Bechtold, M.R. Scheide, J.S. Santos Neto, D. Monteiro de Souza Junior, H. de Campos Braga, L.F.B. Ribeiro, F. Gastaldon, C.T. Pich, T.E.A. Frizon, *Dye. Pigment.* **180**, 108519 (2020)
57. R. Wang, H. Xu, Y. Zhang, Y. Hu, Y. Wei, X. Du, H. Zhao, *Org. Biomol. Chem.* **19**, 5899 (2021)
58. X. Ren, Q. Liu, Z. Yang, Z. Wang, X. Chen, *Chinese Chem. Lett.* **34**, 107821 (2023)
59. C. Ravi, D. Chandra Mohan, S. Adimurthy, *Org. Biomol. Chem.* **14**, 2282 (2016)
60. S. Kundu, B. Basu, *RSC Adv.* **5**, 50178 (2015)
61. Y. An, G. Xu, M. Cai, S. Wang, X. Zhong Wang, Y. Chen, L. Dai, *Tetrahedron* **79**, 131829 (2021)
62. Y.-S. Zhu, Y. Xue, W. Liu, X. Zhu, X.-Q. Hao, M.-P. Song, *J. Org. Chem.* **85**, 9106 (2020)
63. C. Gao, G. Wu, L. Min, M. Liu, W. Gao, J. Ding, J. Chen, X. Huang, H. Wu, *J. Org. Chem.* **82**, 250 (2017)
64. J.M. Anghinoni, S.S. Ferreira, R.F. Schumacher, B.A. Iglesias, G. Perin, F. Penteadó, E.J. Lenardão, *New J. Chem.* **47**, 6066 (2023)

Springer Nature or its licensor (e.g. a society or other partner) holds exclusive rights to this article under a publishing agreement with the author(s) or other rightsholder(s); author self-archiving of the accepted manuscript version of this article is solely governed by the terms of such publishing agreement and applicable law.

Authors and Affiliations

Ke Wang¹ · Li-Yuan Chang² 

✉ Ke Wang
kewang02@163.com

✉ Li-Yuan Chang
liyuanchang839@gmail.com

¹ Baoji University of Arts and Sciences, Baoji 721013, Shaanxi, China

² Institute of Chemical and Nanotechnology Research, Shanghai, China